Journal of Natural Gas Science and Engineering 94 (2021) 104120

Contents lists available at ScienceDirect

Journal of Natural Gas Science and Engineering

journal homepage: www.elsevier.com/locate/jngse

An empirical correlation-based model to predict solid-fluid phase equilibria and phase separation of the ternary system CH_4-CO_2-H_2S

Hani Ababneh, Shaheen A. Al-Muhtaseb *

Department of Chemical Engineering, College of Engineering, Qatar University, 2713, Doha, Qatar

ARTICLE INFO

Keywords:
Natural gas sweetening
Solid phase formation
Ternary mixture separation
Solid-liquid-vapor equilibrium
Freezing prediction
Cryogenic CO_2 separation

ABSTRACT

To cover the expected increased demand for natural gas, energy industry has to exploit sour gas reserves located around the world. However, acid gases have to be removed before the natural gas produced from these fields could be used. One of the novel concepts in this field is the utilization of solid phase formation of carbon dioxide and/or hydrogen sulfide. The main aim of this study is to develop an empirical correlation model based on Peng-Robinson equation of state (PR EoS), with fugacity expressions, that is able for the first time to describe the solid-fluid phase equilibria for the ternary system of CH_4-CO_2-H_2S at pressures from 5 to 30 bar and over a wide range of temperature (130–200 K). The model was first tested on the binary systems of CH_4-CO_2, CO_2-H_2S and CH_4-H_2S with optimized interaction parameters. When proven to be successful, it was then expanded in a predictive manner to describe the ternary system of CH_4-CO_2-H_2S. The model predictions for the solidification points of 5 different mixtures were within the acceptable error when compared to the experimental data available in the literature. A model based on equilibrium stage separation unit was used to study the separation of three different feed compositions of this ternary system. Overall, it was found that separation of CO_2 in solid phase improves when increasing the operating pressure up to 20 bar, and decreases at higher temperatures. Similarly, the separation of H_2S in either liquid or solid phase improves at higher pressures and lower temperatures. The recovery of CH_4 was high over the entire ranges of operating conditions, expect at high pressure (30 Bar) at temperatures below 190 K. This work provides scientists and engineers with an accurate tool that may be used with confidence for predicting solid-fluid phase equilibria. Consequently, this model eliminates difficulties associated with the need for experiments on ternary system solid-fluid phase equilibria.

1. Introduction

In 2019, natural gas accounted for about 25% of the global primary energy consumption (BP, 2020), and it is expected for the natural gas demand to increase by 33% throughout the next 30 years (British Petroleum, 2020). This anticipated increase is due to the discovery of new natural gas and gas condensate fields around the world, in addition to the fact that natural gas has a lower carbon footprint than coal or petroleum products (Theveneau et al., 2020). However, it is estimated that 40% of the proven natural gas fields are sour with high CO_2 and H_2S contents, which could be as high as 70% (Langéet al., 2016) (Kelley et al., 2011). Such acid gases reduce the energy density of the natural gas significantly; hence, lowering its usefulness and selling price. In addition to that, the high content of CO_2 and H_2S can result in corrosion and clogging of pipelines and equipment of liquefaction plants (Maqsood et al., 2014). Thus, the natural gas industry has to look for innovative solutions that make the exploitation of such sour gas reserves economically viable.

Among the most common technologies for acid gas reduction is the post-combustion technique. More specifically, the amine scrubbing technology is the most commonly used method in the industry. However, in addition of being an energy-intensive process, the maintenance and operational costs for amine scrubbing equipment are high due to the corrosivity and volatility of the amine (Wang et al., 2011). On the other hand, low-temperature technologies (such as cryogenic separation) have been applied to for natural gas sweetening. Cryogenic separation is a physical process, which can separate CO_2 and H_2S gases from CH_4 at very low temperatures depending on differences in their volatility (Maqsood et al., 2014). This process has many advantages over the amine absorption process. Such advantages include, but are not limited to, having no solvents required by the process (thus no solvent recovery plants are required) and lower corrosion potentials (Maqsood et al.,

* Corresponding author.
E-mail addresses: ha1805750@student.qu.edu.qa (H. Ababneh), s.almuhtaseb@qu.edu.qa (S.A. Al-Muhtaseb).

https://doi.org/10.1016/j.jngse.2021.104120
Received 23 March 2021; Received in revised form 1 June 2021; Accepted 26 June 2021
Available online 2 July 2021

2014). Additionally, it has a high energetic efficiency (Théveneau et al., 2020). A number of other low-temperature technologies for natural gas sweetening were developed and studied, including the Rectisol process, the dual pressure distillation unit, the Ryan-Holmes process, and the Controlled Freezing Zone (CFZ)™ process (Langéet al., 2016). Depending on the technology in usage, the formation of frozen solids might be desirable or not. From one side, solid phase formation decreases the efficiency of the separation process, and might plug the pipelines and distillation column trays, hence causing potential damage to the equipment (Théveneau et al., 2020). On other hand, some processes, such as CFZ™, utilizes the solid formation in a controlled manner to enhance the separations process, while decreasing the operational costs of the process (Valencia et al., 2014).

To design low-temperature separation processes' units and equipment, experimental data of vapor-liquid equilibrium (VLE), solid-liquid equilibrium (SLE), solid-vapor equilibrium (SVE), and solid-liquid-vapor equilibrium (SLVE) are needed. These experimental data will aid in developing accurate and suitable thermodynamic models, which can predict pressure, temperature and phase compositions of corresponding phase equilibria. The literature contains extensive experimental data and thermodynamics model for the binary systems CO_2-CH_4 (Donnelly and Katz, 1954) (Davis et al., 1962) (Babaret al., 2019) (Tan et al., 2017) (Tang et al., 2019) (Nasrifar and Moshfeghian, 2019), CO_2-H_2S (Chapoy et al., 2013) (Li, 2008) and CH_4-H_2S (Kohn and Kurata, 1958) (Langé et al., 2017) (Cherif, 2016). These literature cover the pressure-temperature (P-T) and temperature-composition (T-x or T-y) diagrams for VLE, SLE, SVE or SLVE loci. However, the equilibrium data involving a solid phase for the ternary system CH_4-CO_2-H_2S are few and limited. Langé et al. have obtained temperature-pressure-composition (T-P-x-y) data for the region in which SLVE exists for different compositions of the CH_4-CO_2-H_2S system. They also tested the reliability of the Yokozeki equation of state (EoS) in predicting their experimental data (Langéet al., 2016). However, their work covers only the region where only one solid phase (i.e., CO_2 solid phase) is present and over limited ranges of temperature (from 199.44 to 207.59 K) and pressure (from 1.4599 to 4.3212 MPa). Theveneau et al. have determined experimentally the temperatures of the solid CO_2 formation for five different mixtures of the ternary system CH_4-CO_2-H_2S (Théveneau et al., 2020), where the feed compositions varied from 63.95 to 79.93 mol% for CH_4 and from 16.04 to 20.07 mol% for CO_2; and the pressure was around 2 MPa. Two equations of state that are based on Group Contribution approach PPR78 (predictive, 1978 Ping Robinson EoS) EoS (Jaubert et al., 2010) and PSRK (Soave–Redlich–Kwong) EoS (Holderbaum and Gmehling, 1991), a semi-empirical EoS, and the PR-HV (Ping Robinson-Huron-Vidal mixing rule) EoS were tested to predict the CO_2 freezing temperatures (Théveneau et al., 2020). The latter model proved to be the most suitable to match the measured equilibrium behavior of the CH_4-CO_2-H_2S system at solidification. Again, this study covered limited ranges of temperature and pressure (192–210 K and 18.48–22.24 Bar); and showed SLVE predictions only at the solidification point.

The main objective of this study is to develop a mathematical model that can describe the solid-fluid phase equilibria for the ternary system of CH_4-CO_2-H_2S over wide ranges of pressure (5–30 bars) and corresponding saturation temperatures, which are not covered in literature; and at different sets of feed compositions. The uniqueness and novelty of this study is that it aims at modelling multiple solid phase formations in various conditions; i.e., VLS_1 (vapor-liquid-solid CO_2) and VS_1S_2 (vapor-solid CO_2-solid H_2S) over a pressure range of 5–30 bars for the ternary system. It is to be noted that, in the studied ranges of pressure and temperature, VLS_2 and VLS_1S_2 are not present due to the inequality of chemical potentials of components in these phases at the specified conditions, which prevents their coexistence at equilibrium. The model will be tested first on the binary systems of CH_4-CO_2, CH_4- H_2S and CO_2-H_2S in a correlative manner (to optimize the corresponding interaction parameters) before its expansion in a predictive manner to the ternary system of CH_4-CO_2-H_2S. The accuracy of the model predictions will be evaluated by comparing its results to the experimental data available in the literature, and it will be examined for different hypothetical feed compositions over wide ranges of pressure and corresponding saturation temperatures. Developing this model accurately helps researchers and the industry by providing them with a useful tool that allows the prediction of the ternary solid-fluid phase equilibrium behavior as well as the separation of such mixtures without the need for experimental data, which in turn optimizes their budget and time.

2. Methodology

This study was conducted in different stages. The first stage was to choose appropriate thermodynamic mathematical model to represent this system. The second stage was to program a code of this thermodynamic model into Aspen Custom Modeller (ACM) V9, which is a process and equipment model development and simulation environment that is based on a programming language code (in the background) that is specific to chemical engineering applications, and involves built-in details of chemical components, their thermophysical properties and process thermodynamics. ACM allows the user to design and build customized process models. So, instead of writing codes, the user write engineering equations that describes such models or equipment, and the ACM provides a powerful tool to execute these models to simulate and optimize continuous, batch, or semi-batch processes.

In order to test the model and confirm its accuracy; the model predictions for the binary mixtures (CH_4-CO_2, CH_4-CO_2 and CO_2-H_2S) are compared to the experimental data available in the literature. Following that, the ACM model was executed at specified number of conditions where experimental data is available for the ternary system CH_4-CO_2-H_2S. Finally, the model was run to obtain phase equilibria and separation performance predictions for the ternary system (CH_4-CO_2-H_2S) over a wide range of operating conditions.

2.1. Modelling

Several approaches are used in the literature to model SLVE systems, including: empirical correlation model (Nikolaidis et al., 2016), thermodynamic integration model proposed by Seiler et al. (2001), Gibbs free energy equation of state for solid CO_2 that is developed by Jäger and Span (Jäger and Span, 2012), and Yokozeki analytical equation of state for solid-liquid-vapor phases (Yokozeki, 2003). The empirical correlation model uses different equations of state for representing the fugacity of the vapor or liquid phases, and another independent model for the fugacity of the solid phase (Tan et al., 2017). The empirical correlation model has shown excellent results and very low deviations from the experimental data for SLVE binary system of CH_4-CO_2 (Nikolaidis et al., 2016); hence it was chosen in this study for modelling the systems in consideration.

2.2. Empirical correlation model

At the phase equilibrium condition of a multicomponent system, the chemical potentials of each component(s) in the two or three coexisting phases (S: solid phase, V/L: vapor and/or liquid phase) at the same temperature (T) and pressure (P), i.e.,

$$\mu_i^S(T,P) = \mu_i^F\left(T,P,\ x^F\right) \tag{1}$$

where μ_i^S is the chemical potential of the component i in a pure solid phase and μ_i^F is the chemical potential of the same component in the coexisting fluid phase (vapor or liquid) with specified molar compositions, x^F. In the case of the reference state being the ideal gas, Eq. (1) can be replaced by (Vera, 2000):

$$\widehat{f}_i^S(T,P) = \widehat{f}_i^F\left(T,P,\ x^F\right) \tag{2}$$

where the solid phase and fluid phase fugacities of component i ($\widehat{f}_i^S$ and $\widehat{f}_i^F$) can be found from Eqs. (3) and (4), respectively (Nikolaidis et al., 2016):

$$\widehat{f}_i^S(T,P) = \widehat{\phi}_{0i}^{Sat}\left(T,\ P_i^{Sub}\right) P_{0i}^{Sat}(T)\ exp\left[\frac{v_{0i}^s}{RT}\left(P - P_{0i}^{Sat}(T)\right)\right] \quad (3)$$

$$\widehat{f}_i^F\left(T,P,\ x^F\right) = x_i^F \widehat{\phi}_i^F\left(T,P,\ x^F\right)P \quad (4)$$

where $P_{0i}^{Sat}(T)$ is the saturation/sublimation pressure of the solid forming component at the specified temperature T, $\widehat{\phi}_{0i}^{Sat}(T,\ P_i^{Sub})$ is the fugacity coefficient of the solid component at temperature T and the saturation pressure P_{0i}^{Sat}, $\widehat{\phi}_i^F(T,P,\ x^F)$ is the fugacity coefficient of the component i in the fluid mixture of molar composition x^F at the temperature T and pressure P, and v_{0i}^s is solid molar volume of the component i.

In order to use Eqs. (2)–(4) for SLVE calculations, an appropriate EoS is selected alongside an equilibrium equation, which estimates the saturation/sublimation pressure of the solid forming component at the given temperature. In this work, Ping-Robinson equation of state (PR EoS) is used (Peng and Robinson, 1929) as illustrated in Section S-5 of the supplementary data file.

2.3. Modelling the binary system of CH_4-CO_2

The first step in this study is to test whether the proposed model can predict the SLVE phase equilibrium at the PT locus curve of the CH_4-CO_2 system. To do so, the model presented in Section S-1 of the supplementary data file is applied.

The accuracy of the model predictions depends on optimizing the interaction parameter (k_{ij}) within the EoS. Thus, several values for the interaction parameter of CH_4-CO_2 system were collected from the published literature. For example, $k_{ij} = 0.1$ (sourced from Nikolaidis et al. (2016)), $k_{ij} = 0.1187$ (sourced from Stringari et al. (2014)), and $k_{ij} = 0.12$ (found in Nasir et al. (2015)). The model predictions are compared to the experimental data found in Davis et al. (1962). The model will be used to estimate the pressure and the composition of each phase at the locus temperature, and the average squared error of these predictions is calculated according to (Kapadia et al., 2017).

$$Error = \frac{\sum\left(\frac{M_{Exp.} - M_{Calculated}}{M_{Exp.}}\right)^2}{N} \quad (5)$$

where M is the property (such as pressure or composition), and N is the number of experimental data points. The k_{ij} value that results in correlated binary data with the least error in pressure and composition (according to Eq. (5)) will be deemed as an optimum interaction parameter; and thus will be adopted for predicting the ternary system equilibria.

2.4. Modelling the binary system of CO_2-H_2S

Similar to the CH_4-CO_2 system, the model is utilized for predicting the solid-fluid phase equilibria of the CO_2-H_2S binary system at the SLVE locus point as described in Section S-2 of the supplementary data file.

Again, several values of the binary interaction parameter between H_2S and CO_2 are utilized for correlating their binary phase equilibrium data that were collected from the published literature. Utilized values involve those reported in literature (such as $k_{ij} = 0.0974$ sourced from Ramdin et al. (2016), $k_{ij} = 0.099$ sourced from Li (2008), and $k_{ij} = 0.095$ found in Chapoy et al. (2013)), and others (i.e., $k_{ij} = 0.0101$, $k_{ij} = 01050$, $k_{ij} = 0.1100$, and $k_{ij} = 0.1200$) that were tested to determine the optimum value for this interaction parameter. The optimum interaction parameter is determined by minimizing the error according to Equation (5).

2.5. Modelling the binary system of CH_4-H_2S

In an independent study conducted by Lange et al. (Langé et al., 2017), they found a non-temperature dependent value for the interaction parameter ($k_{ij} = 0.058$) for the SLVE of the binary system CH_4-H_2S. This value was find to provide satisfactory description of the phase equilibria of the CH_4-H_2S system from 70 K up to the critical temperature of H_2S. No other studies were found to report interaction parameters for this binary system. Thus, this interaction parameter value will be chosen as the starting point to find the optimum interaction parameter value between CH_4-H_2S according to the aforementioned approach. The solid-fluid phase equilibria of this binary system is modeled as described in Section S-3 of the supplementary data file.

2.6. Modelling the ternary system (CH_4-CO_2-H_2S)

To study the SLVE for the ternary system (CH_4-CO_2-H_2S), an equilibrium stage separation unit will be modeled as described in Section S-4 of the supplementary data file. In this unit, a feed stream consisting of the three components (in a specific overall composition) is separated at a certain temperature and pressure into three phases (vapor, liquid and solid). This ternary system (CH_4-CO_2-H_2S) can have two solid phases (namely, a CO_2 solid phase and an H_2S solid phase) over certain ranges of temperature and pressure. It is to be noted that these two solid phases do not always coexist over the entire ranges of pressure and temperature.

The focus of this work will be on the regions where solid phase(s) are in equilibrium with vapor and liquid phases. In this case, two different regions are determined: V-S_1-S_2 (vapor- solid CO_2-solid H_2S), and V-L-S_1 (vapor- liquid-solid CO_2), where S_1 and S_2 refer to the distinct solid phases of pure CO_2 and pure H_2S, respectively, where each of them is assumed to consist of a pure component. It is to be noted that other possible phase combinations (e.g., V-L-S_1-S_2, V-L-S_2, L-S_1, L-S_2, L-S_1-S_2) are not present in the studied ranges of pressure and temperature due to the inequality of chemical potentials of components in these phases at the specified conditions, which prevents their coexistence at equilibrium.

Three phase transition scenarios (the first appearance of vapor phase, the first appearance of S_2 phase and the first appearance of S_1 phase) are investigated. The region where the vapor phase first appears resembles a dew-point region. At that condition, the amount of the output vapor stream (V) in material balances is assumed to be zero; and the set of equations is solved at constant pressure to determine the temperature and compositions of other output streams. Similarly, to find the line where the phase S_2 appears (i.e., phase transition between V-S_1-S_2 and V-L-S_1), S_{H_2S} was set to equal zero at the specified pressure. Finally, the condition when the solid phase (namely, S_1) starts to appear (i.e., the transition line between V-L-S_1 and V-L) was found by setting the value of S_{CO_2} to be zero at the specified pressure. These scenarios allowed determining the various distinct phase regions for this ternary system.

After that, a number of points within each region are tested by solving the appropriate set of equations as presented previously. The performance of the equilibrium stage separation was evaluated by calculating the purity of CH_4 in the vapor phase, the recovery of CH_4 in the vapor phase, the recovery of CO_2 in the solid phase, and recovery of H_2S in either solid or liquid phases. To test the model performance, the feed amount (F) is assumed to equal 1 mol; and three sets of feed compositions were investigated using this model at different conditions. The first set is: $Z_{CH4} = 0.80$, $Z_{CO2} = 0.15$, $Z_{H2S} = 0.05$ (denoted as Case A), the second is: $Z_{CH4} = 0.80$, $Z_{CO2} = 0.10$, $Z_{H2S} = 0.10$ (denoted as Case B), and finally $Z_{CH4} = 0.50$, $Z_{CO2} = 0.30$, $Z_{H2S} = 0.20$ (denoted as Case C).

3. Results and discussion

3.1. Optimization of binary interaction parameters

The optimum interaction parameter (k_{ij}) for the binary system CO_2-H_2S was obtained as described in Section 2.3. Fig. 1a compares the model predictions to the experimental SLVE pressure-temperature data available in the literature (Davis et al., 1962), while Fig. 1b further compares the distribution of CO_2 between phases as a function of temperature. Table 1 shows the calculated average squared errors between model predictions at the specified k_{ij} values and the experimental data in terms of pressure and CO_2 composition. It could be noticed that k_{ij} = 0.1200 has the best results as it produces the lowest sum of errors, hence providing best correlation to the experimental data. Thus, it is recommended to use this interaction parameter value between CH_4 and CO_2 for any further calculations involving these two components. It could be concluded from Fig. 1 that the model predictions can describe experimental data available in the literature very well, hence indicating the possibility of building over this ACM model for modelling other systems involving these two components, such as the ternary system CH_4-CO_2-H_2S.

The optimum interaction parameter (k_{ij}) for the binary system CO_2-H_2S was obtained as described in Section 2.4. Table 2 shows the calculated average squared errors between model predictions at the specified k_{ij} values and experimental data in terms of pressure and H_2S compositions (Sobocinski and Kurata, 1959). From Table 2, it is concluded that the k_{ij} = 0.1100 produces the least sum of average squared errors when compared to the other values. Thus, k_{ij} = 0.1100 is considered as an optimum interaction parameter for this binary system, and will be adopted for further calculations involving the components H_2S and CO_2. Once again, the model proved successful in predicting the SLVE Pressure-Temperature locus and compositions as seen in Fig. 2.

Combining the results of the two binary systems (CO_2-CH_4 and H_2S-CO_2) produces Fig. 3, which is calculated at the optimum interaction parameter found for each binary system. Fig. 3 shows that the loci curves of the models meets at the estimated triple point of pure CO_2 (215.8 K, 4.9 bar), which is slightly different from the actual triple point of CO_2 (216.5 K, 5.2 bar) (Schneider, 1977).

The optimum interaction parameter (k_{ij}) for the binary system CH_4-H_2S was obtained as described in section 2.5. Table 3 shows the calculated average squared errors between model predictions at the specified k_{ij} values and experimental data (Kohn and Kurata, 1958) in terms of SLVE pressures and Quadruple point (QP) pressure. It is concluded that the k_{ij} = 0.058 results in the least sum of average squared errors. Thus, it is considered as an optimum interaction parameter for this binary system, and will be adopted for further calculations involving the components H_2S and CH_4. Similar to the previous two systems, the model proved to be successful in predicting the SLVE Pressure-Temperature locus for this binary system as illustrated in Fig. 4.

Table 1
Effect of selected interaction parameter on the average squared errors in predicting SVLE pressures and CO_2 compositions in the binary system: CH_4-CO_2. Data with bold font indicate optimum interaction parameter with the least sum of errors.

k_{ij}	Error in Pressure	Error in x_{CO_2}	Error in y_{CO_2}	Sum of errors
0.1000	0.0017	0.0451	0.0668	0.1136
0.1187	0.0297	0.0115	0.0711	0.1123
0.1200	**0.0010**	**0.0143**	**0.0668**	**0.0821 (min)**
0.1250	0.0023	0.0208	0.0715	0.0946

Table 2
Effect of selected interaction parameter on the average squared errors in predicting SVLE pressures and H_2S compositions in the binary system: H_2S-CO_2. Data with bold font indicate optimum interaction parameter with the least sum of errors.

k_{ij}	% Error in Pressure	%Error in x_{H_2S}	%Error in y_{H_2S}	%Sum of errors
0.0950	0.26	4.06	11.47	15.79
0.0974	0.25	4.02	11.13	15.40
0.0990	0.25	4.02	10.9	15.17
0.1010	0.25	4.04	10.6	14.89
0.1050	0.24	4.18	10.10	14.52
0.1100	**0.24**	**4.57**	**9.29**	**14.10 (min)**
0.1200	0.23	6.28	8.56	15.07

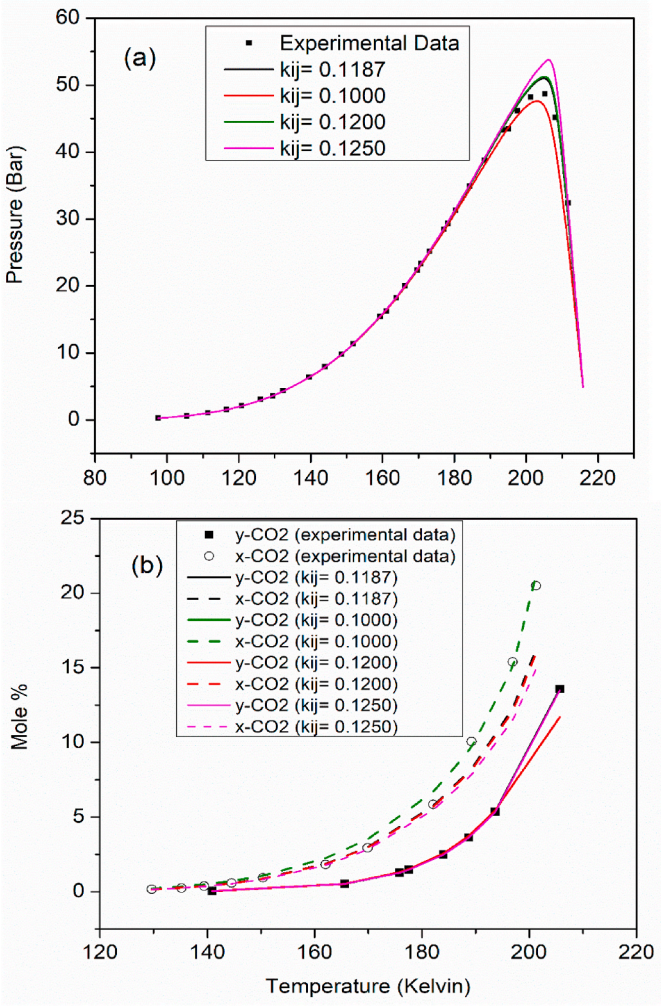

Fig. 1. Comparison of model predictions and experimental data for the binary system of CO_2 and CH_4. Subfigures show the effect of temperature on equilibrium (a) pressure and (b) composition of CO_2 in each phase.

3.2. Modelling results of the ternary system: CH_4-CO_2-H_2S

Pascal et al. (Théveneau et al., 2020) have used a visual synthetic experimental method to find the solidification point for five compositions of the ternary mixture CH_4-CO_2-H_2S. The compositions of these mixtures are listed in Table 4. These data were also predicted in this work using the previously presented model with the optimized interaction parameters between each pair of components as determined in the previous section. The Mean Absolute Deviation (MAD) (Eq. (6)) between the measured and predicted solidification temperatures is 2.86 K and the Mean Relative Deviation (MRD) (Eq. (7)) is 1.44%, indicating that the model has successfully predicted the solidification temperature for a these mixtures.

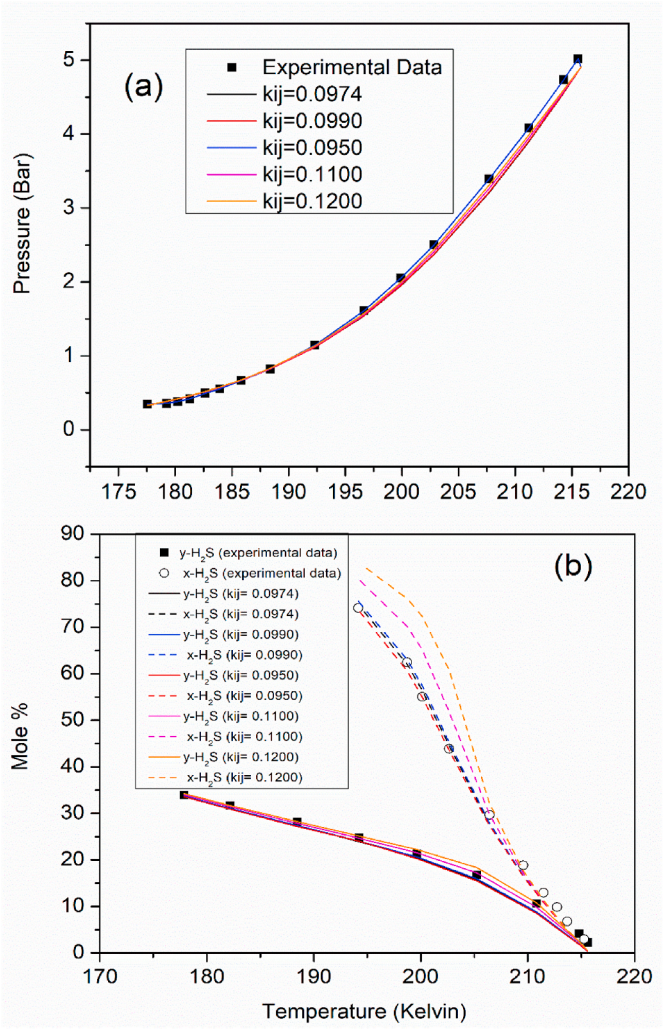

Fig. 2. Comparison of model predictions and experimental data for the binary system of CO_2 and H_2S. Subfigures show the effect of temperature on equilibrium (a) pressure and (b) composition of H_2S in each phase.

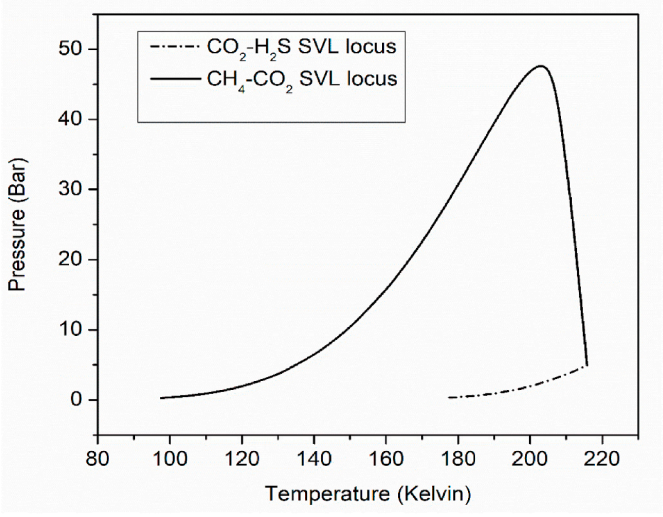

Fig. 3. Combined SLVE P-T loci correlations for the binary systems of CH_4-CO_2 and CO_2-H_2S.

Table 3
Effect of interaction parameter on the average squared errors in predicting SLVE pressures and the quadruple point pressures in the binary system: H_2S-CH_4. Data with bold font indicate optimum interaction parameter with the least sum of errors.

k_{ij}	Error in QP	Error in SVL_1E	Error in SVL_2E	(Sum of errors)/3
0.100	9.351	1.002	287.248	99.200
0.070	11.790	0.864	221.656	78.103
0.058	**15.664**	**1.824**	**155.581**	**57.690 (min)**
0.040	25.616	3.592	252.336	93.848

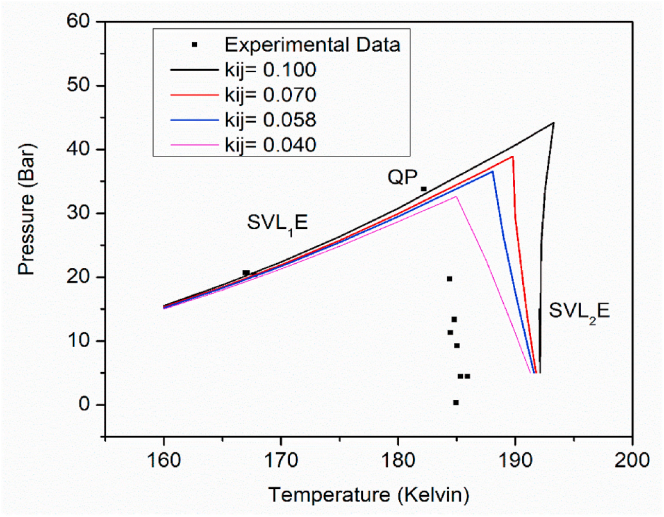

Fig. 4. Comparison of model predictions and experimental data for the effect of temperature on equilibrium behavior of the binary system of CH_4 and H_2S. Symbols before and after QP correspond, respectively, to SVL_1E and SVL_2E.

Table 4
Comparison between experimental and predicted temperatures of solidification for various compositions, and errors in predicted temperatures.

Mixture	Z_{CH4}	Z_{CO2}	Z_{H2S}	P (MPa)	T_{exp} (Kelvin)	T_{pred} (Kelvin)
1	0.7993	0.2007	0	2.224	209.80	213.03
2	0.7603	0.1899	0.0498	2.186	202.33	203.74
3	0.7192	0.1806	0.1002	1.848	196.85	200.05
4	0.6802	0.1701	0.1497	1.974	194.32	197.62
5	0.6395	0.1604	0.2001	2.123	192.26	195.43
MAD (K)				2.86		
MRD (%)				1.44%		

$$MAD = \frac{1}{N}\sum\left|U_{cal} - U_{exp}\right| \tag{6}$$

$$MRD = \frac{100}{N}\sum\left|\frac{U_{cal} - U_{exp}}{U_{exp}}\right| \tag{7}$$

where U is the property, cal is the value estimated by the model, and exp is the experimental data.

Since the model has proved to be sufficiently accurate and reliable, the model was run to study the SLVE and separation performances for the 3 different of compositions (cases A, B and C) as mentioned in section 2.6 and listed in Table 5. Table 5 also indicate that the corresponding composition ratios of CO_2/CH_4, H_2S/CH_4 and H_2S/CO_2 follow the trends B < A < C, A < B < C and A < C < B, respectively. The phase diagrams (Pressure-Temperature diagram) for the three cases are shown in Fig. 5a, b, and 5c respectively; while Fig. 5d shows the overlaid phase diagrams of three cases on the same graph. Fig. 5a, b, and 5c also show the points

Table 5
CO_2/CH_4, H_2S/CH_4 and H_2S/CO_2 ratios for each case of the feed.

Case	Z_{CH4}	Z_{CO2}	Z_{H2S}	CO_2/CH_4	H_2S/CH_4	H_2S/CO_2
A	0.80	0.15	0.05	0.1875	0.0625	0.333
B	0.80	0.10	0.10	0.1250	0.1250	1.000
C	0.50	0.30	0.20	0.6000	0.4000	0.667

tested to collect data for compositions, recovery, and products distribution.

By studying the phase diagrams for the three cases, it could be noticed that the line between the L-S_1-S_2 and V-S_1-S_2/V-L-S_1 regions (indicating the first appearance of the vapor phase) follows the same trend for the three cases till the point where the three regions (L-S_1-S_2, V-S_1-S_2, and V-L-S_1) regions meet, which indicates the point where the four phases (V-L-S_1-S_2) coexist. After that point the lines behave differently for each case. From Fig. 5d and Table 5, it could be concluded that increasing the ratio of H_2S/CH_4 in the feed (which follows the sequence A < C < B) results in a smaller V-L-S_1 region (that follows the sequence A > C > B); with a lower temperature for coexistence of these four phases; where this temperature follows the sequence A < B < C (following the H_2S/CH_4 composition ratio). Similarly, the trend of the V-L-S_1/V-L equilibrium lines (which resemble the melting condition of the solid phase) trend is governed by the H_2S/CO_2 ratio, where it can be seen that the melting temperatures sequence is (B < C < A); which follows the opposite sequence of H_2S/CO_2 ratio (B > C > A). In other words, lower H_2S/CO_2 ratios would move the curve to the right (higher melting temperature at the same pressure). The H_2S/CH_4 ratio (which follows the order A < B < C) also impacts the V-S_1-S_2/V-L-S_1 equilibrium line. Higher H_2S/CH_4 ratios in the feed would move the line upward (vertically) and make the V-S_1-S_2 region larger. This phenomenon could be explained by the fact that H_2S solidification temperature is higher than that of CH_4, thus increasing its amount in the feed would move the line to higher temperature.

The effect of temperature on vapor phase compositions of CH_4 and CO_2 at different pressures are shown in Fig. 6a, b and 6c for cases A, B and C, respectively. In general, higher temperatures result in reducing y_{CH_4}, and increasing y_{CO_2} and y_{H_2S}. However, higher pressures at the same temperature increases y_{CH_4} and reduces y_{CO_2} and y_{H_2S}. Overall, highest CH_4 purities in the vapor phase can be obtained when reducing temperature and or pressure. Furthermore, the effect of feed composition has a negligible effect on y_{CH_4} and y_{CO_2} at the same temperature and pressure.

The effects of temperature and pressure on the liquid phase composition are shown in Fig. 7. On one hand, temperature has insignificant impact on x_{CH_4} except at high pressure (30 Bar), where high temperature would result in reducing x_{CH_4} significantly. On the other hand, increasing the pressure at constant temperatures increases x_{CH_4}. Furthermore, x_{CO_2} and x_{H_2S} increase when increasing either pressure or temperature. Furthermore, it seems that the feed composition has no significant impact on the x_{CH_4} value, while increasing the H_2S/CH_4 ratio (which follows the sequence A < B < C) will results in higher x_{CO_2} and lower x_{H_2S} at the same pressure and temperature.

To study the performance of the equilibrium stage separation; the effects of temperature and pressure on the recovery of CH_4 in the vapor phase, the recovery of CO_2 in the solid phase, and the recovery of H_2S in the liquid/solid phases are investigated as shown in Figs. 8 and 9, and 10, respectively. The recovery of a component in a certain phase is calculated as the ratio of the moles of that component in the specified phase relative to the moles of that component in the feed mixture.

Fig. 8 shows that the CH_4 recovery in the vapor phase does not change significantly with operating temperatures and pressures; except at high pressure (30 Bar) and low temperature (190> K); where it drops to ~0% at ~180 K. This could be attributed to the fact that the vapor

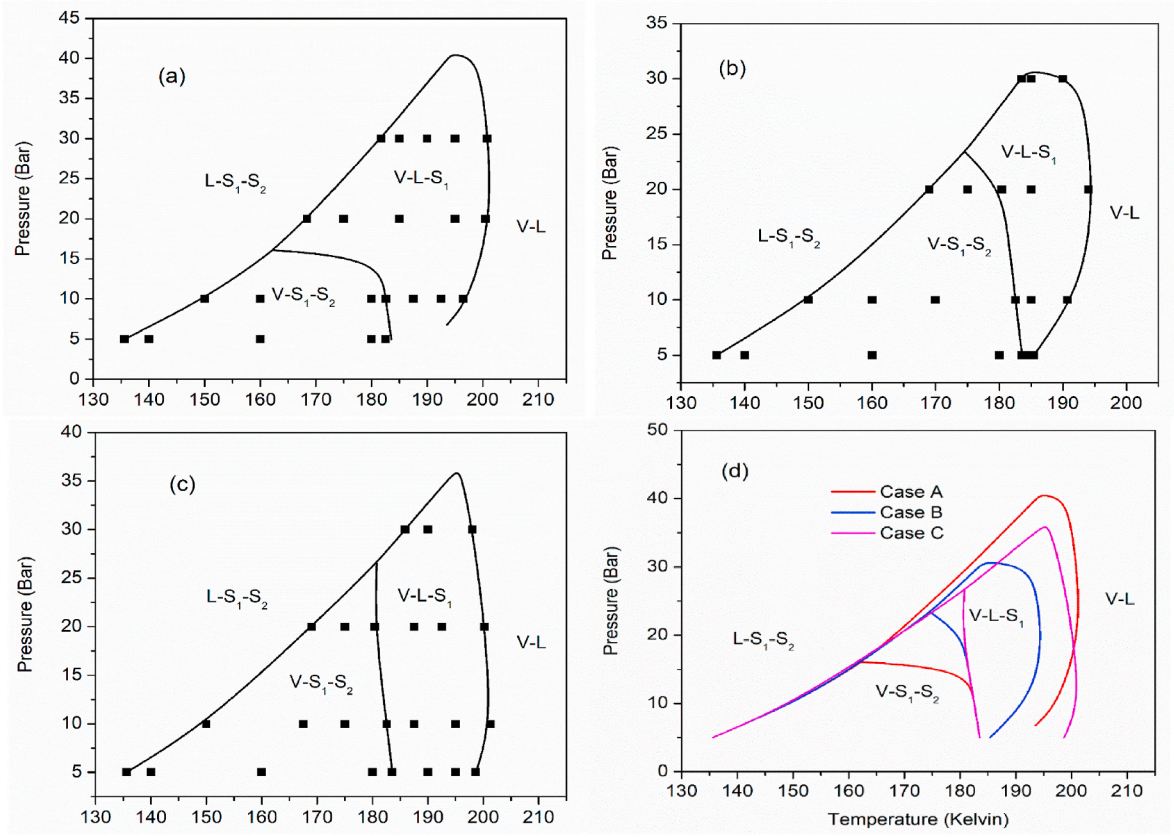

Fig. 5. Pressure-Temperature phase diagrams for (a) Case A, (b) Case B, (c) Case C, and (d) comparison of the three cases. Symbols (■) indicate points tested to collect data for compositions, recovery, and products distribution for the cases listed in Table 5.

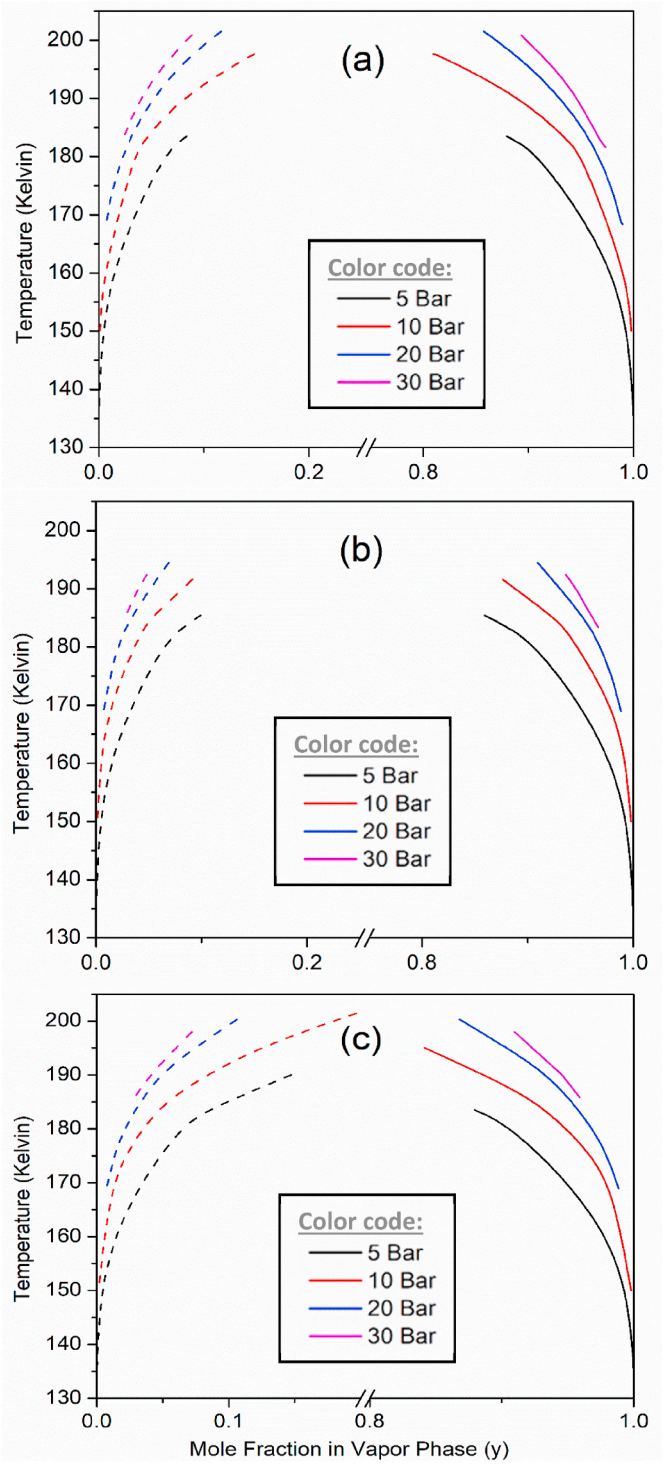

Fig. 6. Effects of temperature and pressure on the vapor phase compositions of CH_4 (solid lines) and CO_2 (dashed lines) in Cases (a) A, (b) B and (c) C. Different colors indicate pressure values as illustrated in the legends.

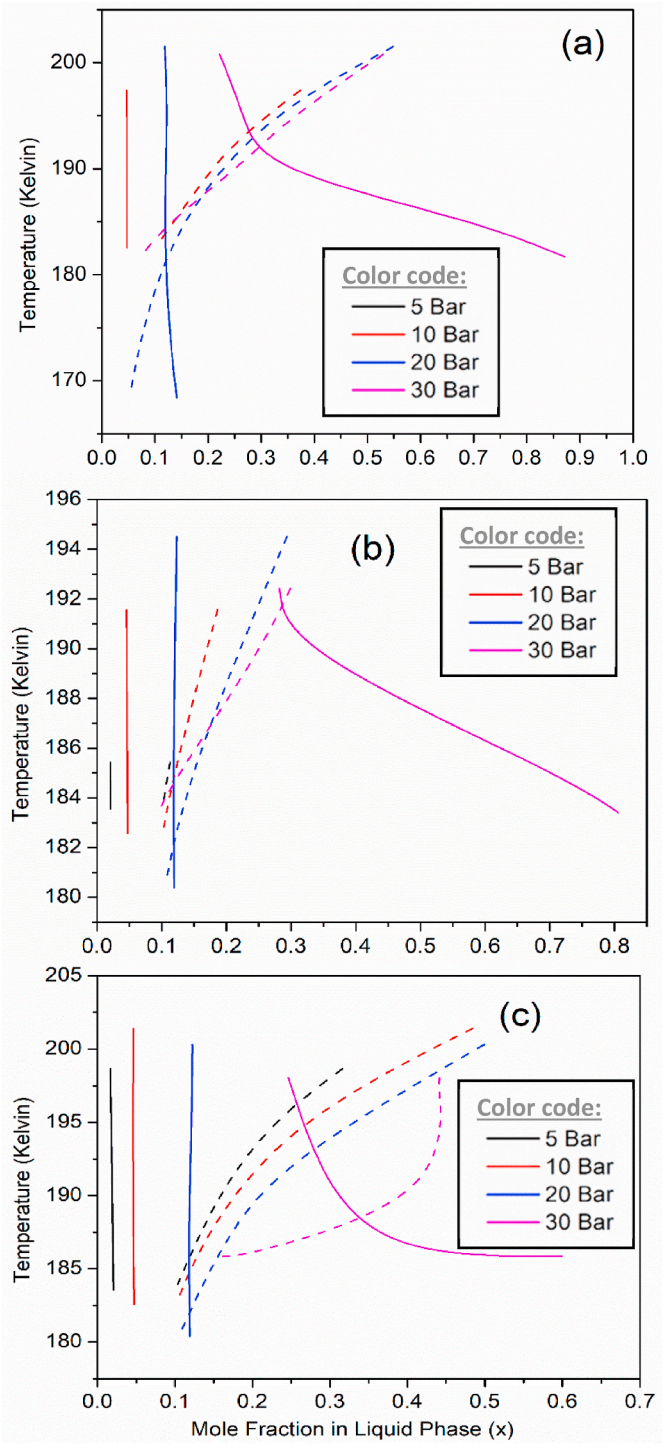

Fig. 7. Effects of temperature and pressure on the liquid phase compositions of CH_4 (solid lines) and CO_2 (dashed lines) in Cases (a) A, (b) B and (c) C. Different colors indicate pressure values as illustrated in the legends.

phase amount drops significantly at these conditions as seen later in Fig. 11, despite the fact that y_{CH_4} increases with the increase in temperature and pressure. Overall, the CH_4 recovery in the vapor phase exceeded 90% in all cases expect the one mentioned above, and will be 100% in the operating region of VS_1S_2. The feed composition has a minimal impact on the CH_4 recovery in the VS_1S_2 region (low temperatures and pressures); whereas in the VLS_1 region, increasing the H_2S ratio in the feed will reduce the recovery of CH_4 in the vapor phase.

Fig. 9 shows that the CO_2 recovery in the solid phase decreases when increasing temperatures. However, at a constant temperature, it increases when increasing in the operating pressure up to pressure of 20 bar, after which the CO_2 recovery will decrease. Having more CO_2 in the feed (higher CO_2/CH_4 ratio) will improve the CO_2 recovery in the solid phase noticeably at the same operating conditions.

Fig. 10 illustrates the H_2S recovery in the three studied cases in liquid and solid phases. Overall, it is clear that the H_2S recovery increasing when reducing the operating temperature and/or increasing the

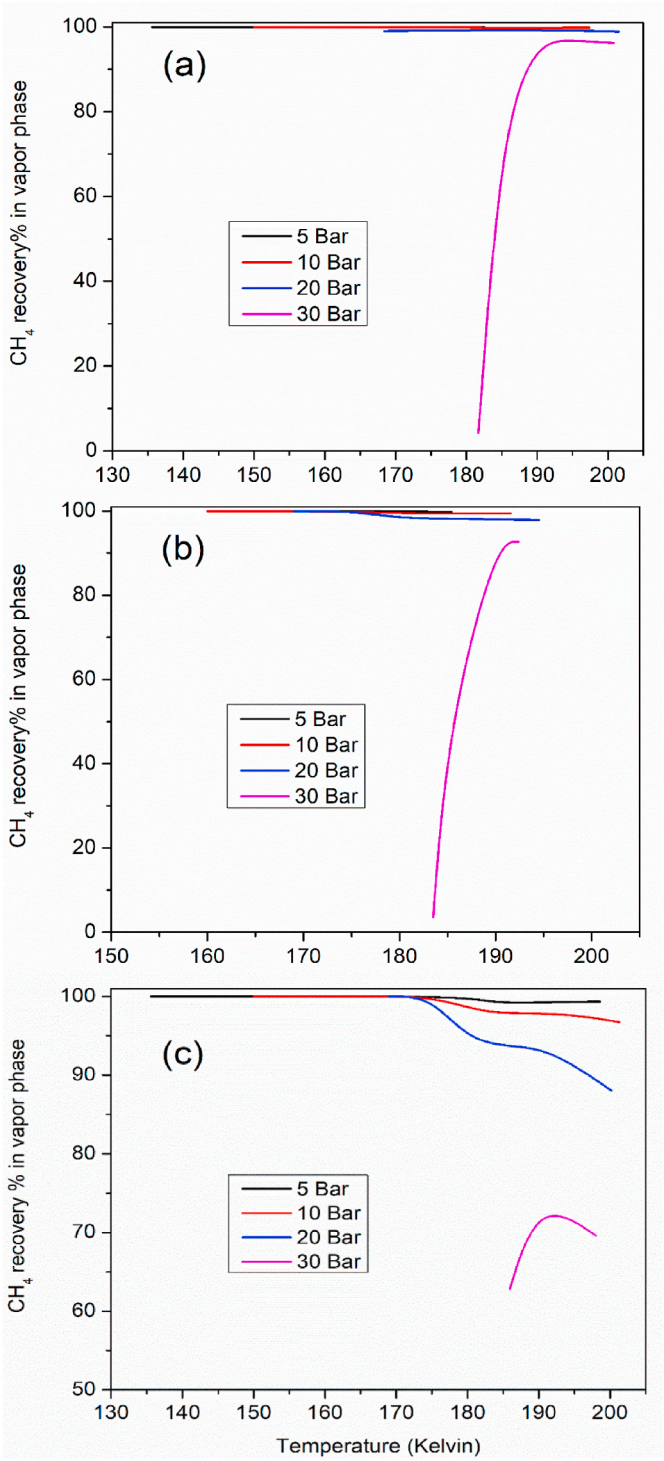

Fig. 8. Effects of temperature and pressure on the vapor-phase recovery (%) of CH_4 in Cases (a) A, (b) B and (c) C. Different colors indicate pressure values as illustrated in the legends.

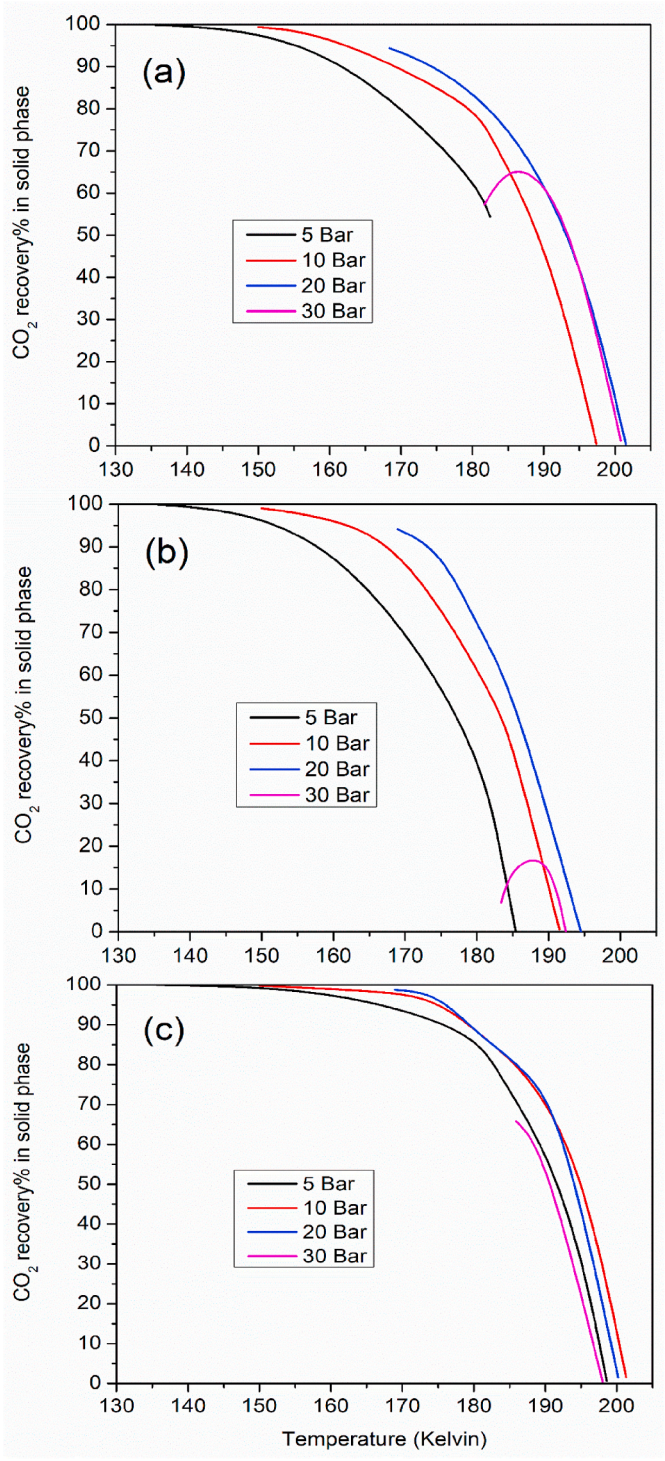

Fig. 9. Effects of temperature and pressure on the solid-phase recovery of CO_2 in Cases (a) A, (b) B and (c) C. Different colors indicate pressure values as illustrated in the legends.

operating pressure. Therefore, higher operating pressures will improve the separation of both CO_2 (in the solid phase) and H_2S (in solid and liquid phase) but it will decrease CH_4 recovery in the vapor phase. Thus, it is important to determine the priorities in separation to determine the desired separation conditions. The feed composition has no clear impact on the H_2S recovery in the liquid phase. However, the model predictions indicate that higher H_2S/CH_4 ratios in the feed will improve the recovery of H_2S in the solid phase. In general, the best region to separate the ternary system components can be the region of VS_1S_2 at the highest possible pressure and temperature.

Fig. 11 illustrates the impact of temperature and pressure on the V/F and S_{CO_2}/F phase ratios resulting from each of the studied cases. Increasing the temperature will increase V/F ratio, but it will decrease S_{CO_2}/F, S_{H_2S}/F and L/F phase ratios. The relationship between the pressure and the produced phase ratios is opposite; increasing pressure lowers the V/F ratio and increases the S_{CO_2}/F, S_{H_2S}/F and L/F phase

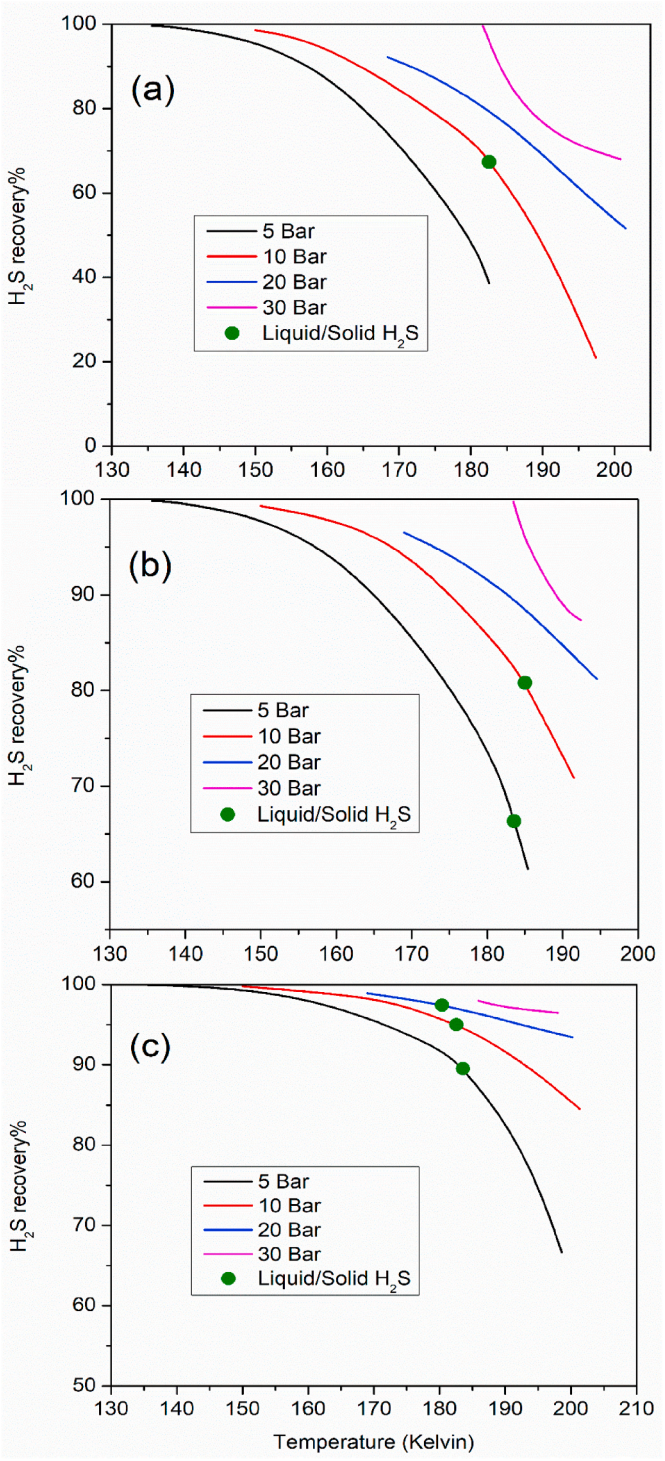

Fig. 10. Effects of temperature and pressure on the recovery of H_2S in solid and liquid phases in Cases (a) A, (b) B and (c) C. Symbols (●) indicate the transition points between solid and liquid phases at each pressure. Different colors indicate pressure values as illustrated in the legends.

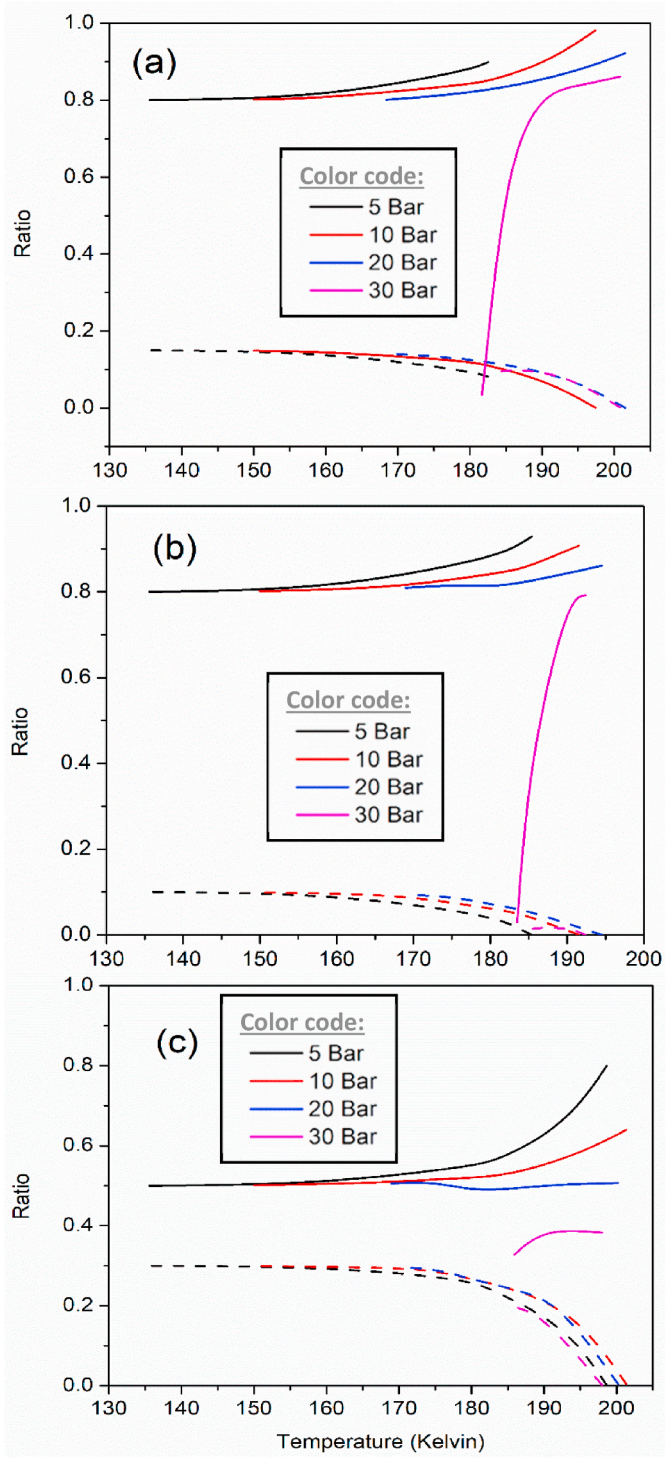

Fig. 11. Effects of temperature and pressure on the V/F and S_{CO_2}/F phase ratios (solid and dashed lines, respectively) in Cases (a) A, (b) B and (c) C. Different colors indicate pressure values as illustrated in the legends.

ratios. Increasing the CO_2/CH_4 ratio in the feed will raise the produced S_{CO_2}/F ratio (i.e., it will follow the sequence B < A < C). Similarly, increasing the H_2S/CH_4 ratio will increase the produced ratio (i.e., it will follow the sequence A < B < C). Fig. 11c shows that case C has the lowest V/F ratio compared to other two cases at similar operating conditions, this might be explained by the lowest CH_4 composition in the feed compared to the other two cases (0.5 vs. 0.8). Furthermore, there was no clear relation between the feed compositions and the produced L/F phase ratios.

4. Conclusions

In this study, an empirical phase equilibrium correlation model based on Peng-Robinson equation of state (PR EoS) with fugacity expressions was developed to describe the solid-fluid phase for the ternary system of CH_4-CO_2-H_2S over a wide ranges of pressure (5–30 bars) and

temperature (130–200 K); and at different sets of feed compositions. The model was first tested on the binary systems CH_4-CO_2, CH_4-H_2S and CO_2-H_2S; and was found successful in predicting the corresponding solidification points and their compositions when optimizing the corresponding interaction parameters. Therefore, it was further expanded in a predictive manner to the ternary system CH_4-CO_2-H_2S. The model's predictions for the solidification points for this ternary mixture with five different compositions were within the acceptable error limits (with an absolute mean deviation of 2.86 K in solidification temperature) when compared to the experimental data available in the literature. An equilibrium stage separation unit was used to study the separation of three different feed compositions of the ternary system CH_4-CO_2-H_2S based on the model developed in this work. Overall, it was found that separation of CO_2 improves when increasing the operating pressure up to 20 bar and decreases at higher temperatures. Similarly, the separation of H_2S improves at higher pressures and decreases at elevated temperatures. The recovery of CH_4 was high over the entire operating conditions ranges, expect at high pressure (30 Bar) and temperature (190> K). The success of the model in predicting solid-fluid phase equilibria of this ternary system makes it a useful tool for engineers and researchers to understand the pertaining behaviors and design corresponding separation processes for the natural gas industry.

Authors' contributions

Hani Ababneh: Conceptualization, Investigation, Work Execution, Methodology, Software, Writing – original draft. Shaheen A. Al-Muhtaseb: Conceptualization, Investigation, Methodology, Supervision, Validation, Writing - reviewing and editing.

Availability of data and material

All data generated or analyzed during this study are included in this article.

Funding

Not applicable.

Declaration of competing interest

The authors declare that they have no known competing financial interests or personal relationships that could have appeared to influence the work reported in this paper.

Acknowledgements

The publication of this article was funded by the Qatar National Library.

Appendix A. Supplementary data

Supplementary data to this article can be found online at https://doi.org/10.1016/j.jngse.2021.104120.

References

Babar, M., et al., 2019. Thermodynamic data for cryogenic carbon dioxide capture from natural gas: a review. Cryogenics 102, 85–104. https://doi.org/10.1016/j.cryogenics.2019.07.004. June.

British Petroleum, 2020. Energy Outlook 2020. https://www.bp.com/content/dam/bp/business-sites/en/global/corporate/pdfs/energyeconomics/energy-outlook/bp-energy-outlook-2020.pdf. (Accessed 15 December 2020).

Chapoy, A., Coquelet, C., Liu, H., Valtz, A., Tohidi, B., 2013. Vapour-liquid equilibrium data for the hydrogen sulphide (H2S)+carbon dioxide (CO2) system at temperatures from 258 to 313K. Fluid Phase Equil. 356, 223–228. https://doi.org/10.1016/j.fluid.2013.07.050.

Cherif, H., 2016. Study and modeling of separation methods H2S from methane , selection of a method favoring H2S valorization. Univ. Paris Sci. Lett.

Davis, J.A., Rodewald, N., Kurata, F., 1962. "Solid-liquid-vapor phase behavior of the methane-carbon dioxide system. AIChE J. 8 (4), 537–539. https://doi.org/10.1002/aic.690080423.

Donnelly, H.G., Katz, D.L., 1954. "Phase equilibria in the carbon dioxide–methane system. Ind. Eng. Chem. 46 (3), 511–517. https://doi.org/10.1021/ie50531a036.

Holderbaum, T., Gmehling, J., 1991. PSRK: a Group contribution equation of state based on UNIFAC. Fluid Phase Equil. 70 (2), 251–265. https://doi.org/10.1016/0378-3812(91)85038-V.

Jäger, A., Span, R., 2012. Equation of state for solid carbon dioxide based on the Gibbs free energy. J. Chem. Eng. Data 57 (2), 590–597. https://doi.org/10.1021/je2011677.

Jaubert, J.-N., Privat, R., Mutelet, F., 2010. Predicting the phase equilibria of synthetic petroleum fluids with the PPR78 approach. AIChE J. 56 (12), 3225–3235. https://doi.org/10.1002/aic.12232. Dec.

Kapadia, A.S., Chan, W., Moyé, L., 2017. Mathematical Statistics with Applications, seventh ed. Thomson.

Kelley, B.T., Valencia, J.A., Northrop, P.S., Mart, C.J., 2011. Controlled Freeze ZoneTM for developing sour gas reserves. Energy Procedia 4, 824–829. https://doi.org/10.1016/j.egypro.2011.01.125.

Kohn, J.P., Kurata, F., 1958. "Heterogeneous phase equilibria of the methane—hydrogen sulfide system. AIChE J. 4 (2), 211–217. https://doi.org/10.1002/aic.690040217.

Langé, S., Campestrini, M., Stringari, P., Langé, S., Campestrini, M., Stringari, P., 2017. Phase behavior of system methane + hydrogen sulfide. AIChE J. 62 (11), 4090–4108.

Langé, S., et al., 2016. Experimental de- termination OF the solid-liquid-vapor locus for the CH 4 -CO 2 -H 2 S system And application to the design OF a new low-temperature distillation process for the purification OF natural gas. In: 94th GPA Convention.

Li, H., 2008. "Thermodynamic Properties of CO2 Mixtures and Their Applications in Advanced Power Cycles with CO2 Capture Processes.

Maqsood, K., Mullick, A., Ali, A., Kargupta, K., Ganguly, S., 2014. Cryogenic carbon dioxide separation from natural gas: a review based on conventional and novel emerging technologies. Rev. Chem. Eng. 30 (5), 453–477. https://doi.org/10.1515/revce-2014-0009.

Nasir, Q., Sabil, K.M., Lau, K.K., 2015. Measurement of isothermal (vapor+liquid) equilibria, (VLE) for binary (CH4+CO2) from T=(240.35 to 293.15) K and CO2 rich synthetic natural gas systems from T=(248.15 to 279.15) K,. J. Nat. Gas Sci. Eng. 27, 158–167. https://doi.org/10.1016/j.jngse.2015.08.045.

Nasrifar, K., Moshfeghian, M., 2019. Prediction of carbon dioxide frost point for natural gas and LNG model systems. J. Nat. Gas Sci. Eng. 76, 103206. https://doi.org/10.1016/j.jngse.2020.103206, 2020.

Nikolaidis, I.K., Boulougouris, G.C., Peristeras, L.D., Economou, I.G., 2016. Equation-of-State modeling of solid-liquid-gas equilibrium of CO2 binary mixtures. Ind. Eng. Chem. Res. 55 (21), 6213–6226. https://doi.org/10.1021/acs.iecr.6b00669.

Peng, D., Robinson, D.B., 1929. A new equation of state. Nature 123 (3100), 507.

Ramdin, M., Becker, T.M., Jamali, S.H., Wang, M., Vlugt, T.J.H., 2016. Computing equation of state parameters of gases from Monte Carlo simulations. Fluid Phase Equil. 428, 174–181. https://doi.org/10.1016/j.fluid.2016.06.012.

Schneider, G.M., 1977. Book Review: carbon Dioxide – international Thermodynamic Tables of the Fluid State, Bd. 3. Von S. Angus, B. Armstrong und K. M. de Rerrck. Pergamon Press Ltd., Oxford–New York 1976. Chem. Ing. Tech. 49, 594. https://doi.org/10.1002/cite.330490727.

Seiler, M., Groß, J., Bungert, B., Sadowski, G., Arlt, W., 2001. Modeling of solid/fluid phase equilibria in multicomponent systems at high pressure. Jun Chem. Eng. Technol. 24 (6), 607–612. https://doi.org/10.1002/1521-4125, 200106)24:6<607::AID-CEAT607>3.0.CO;2-T.

Sobocinski, D.P., Kurata, F., 1959. "Heterogeneous phase equilibria of the hydrogen sulfide–carbon dioxide system. AIChE J. 5 (4), 545–551. https://doi.org/10.1002/aic.690050425.

Stringari, P., Campestrini, M., Coquelet, C., Arpentinier, P., 2014. An equation of state for solid-liquid-vapor equilibrium applied to gas processing and natural gas liquefaction. Fluid Phase Equil. 362, 258–267. https://doi.org/10.1016/j.fluid.2013.10.020.

Tan, Y., Nookuea, W., Li, H., Thorin, E., Yan, J., 2017. Cryogenic technology for biogas upgrading combined with carbon capture-a review of systems and property impacts. Energy Procedia 142, 3741–3746. https://doi.org/10.1016/j.egypro.2017.12.270.

Tang, L., Li, C., Lim, S., 2019. Solid-liquid-vapor equilibrium model applied for a CH4-CO2 binary mixture. Ind. Eng. Chem. Res. 58 (39), 18355–18366. https://doi.org/10.1021/acs.iecr.9b02389.

Theveneau, P., Xu, X., Baudouin, O., Jaubert, J.N., Ceragioli, P., Coquelet, C., 2020. Vapor-liquid equilibria of the CH4 + CO2 + H2S ternary system with two different global compositions: experiments and modeling. J. Chem. Eng. Data 65 (4), 1802–1813. https://doi.org/10.1021/acs.jced.9b01082.

Théveneau, P., Fauve, R., Coquelet, C., Mougin, P., 2020. "Measurement and modelling of solid apparition temperature for the CO2 – H2S – CH4 ternary system. Fluid Phase Equil. 509, 112465. https://doi.org/10.1016/j.fluid.2020.112465.

Valencia, J.A., Denton, R.D., Northrop, P.S., Mart, C.J., Smith, R.K., 2014. Controlled freeze zone technology for the commercialization of Australian high CO2 natural gas. Soc. Pet. Eng. - SPE Asia Pacific Oil Gas Conf. Exhib. APOGCE 2014 - Chang. Game Oppor. Chall. Solut. 2, 951–961. https://doi.org/10.2118/171508-ms.

Vera, J.H., 2000. Book review: molecular thermodynamics of fluid-phase equilibria by John M. Prausnitz, Rüdiger N. Lichtenthaler and Edmundo Comes de Azevedo, Third edition. Can. J. Chem. Eng. 78 (2), 429–430. https://doi.org/10.1002/cjce.5450780222, 1999.

Wang, M., Lawal, A., Stephenson, P., Sidders, J., Ramshaw, C., 2011. Post-combustion CO2 capture with chemical absorption: a state-of-the-art review. Chem. Eng. Res. Des. 89 (9), 1609–1624. https://doi.org/10.1016/j.cherd.2010.11.005.

Yokozeki, A., 2003. Analytical equation of state for solid-liquid-vapor phases. Int. J. Thermophys. 24 (3), 589–620. https://doi.org/10.1023/A:1024015729095.

BP, 2020. Statistical Review of World Energy 2020. https://www.bp.com/content/dam/bp/business-sites/en/global/corporate/pdfs/energyeconomics/statistical-review/bp-stats-review-2020-full-report.pdf. (Accessed 10 December 2020).